Nuclear Materials and Energy 39 (2024) 101659

Contents lists available at ScienceDirect

Nuclear Materials and Energy

journal homepage: www.elsevier.com/locate/nme

Production of ^{165}Er with deuterons at IFMIF-DONES

E. López-Melero [a,*], F. Arias de Saavedra [a], I. Da Silva [b], A. Roldán [c], J. Praena [a]

[a] Department of Atomic, Molecular and Nuclear Physics, University of Granada, E-18071, Granada, Spain
[b] Conditions Extremes Materiaux: Haute Temperature et Irradiation, UPR 3079 CNRS, Université d' Orléans, F-45071, Orléans, France
[c] Department of Electronics and Computer Technology, University of Granada, E-18071, Granada, Spain

ARTICLE INFO

Keywords:
^{165}Er direct route production
Deuteron beam
Auger-electron therapy
SolidWorks

ABSTRACT

The production of radioisotopes for nuclear medicine is boosted by different international agencies. IFMIF-DONES will be an infrastructure where neutrons will be generated by the impact of a high-power deuteron beam onto a lithium jet target. At present, IFMIF-DONES studies the possibility of deflecting 0.1% of its standard 125 mA current of 40 MeV deuteron beam for the complementary applications to be conducted inside a new experimental hall. Such deuteron beam is being considered to be used for radioisotope production for nuclear medicine. Here, we discuss the production of a potential Auger-electron emitter radioisotope for therapy^{165}Er with 125 μA deuterons on ^{nat}Ho. Due to the high-power delivered onto the sample, we study by means of SolidWorks simulations a realistic device as cooling system for the holmium sample. Our results show a significant^{165}Er production in comparison with other experimental routes available in the literature.

1. Introduction

The use of compounds and biomolecules labelled with radionuclides obtained from rare earth elements has grown in nuclear medicine. The biologic properties similar to those of lanthanides have been the basis for research into therapeutic applications. [1]. The success of ^{177}Lu in therasnostics is an excellent example of this tendency [2]. ^{177}Lu is incorporated to different molecules as ^{177}Lu-DOTATATE [2], ^{177}Lu-PSMA [3] or ^{177}Lu-AntiHER2 [4]. Auger electron (AE) emitters are characterized by energies in the range of 0.02–50 keV, a short tissue penetration range of 0.0007 to 40 μm, and a high linear energy transfer (LET) of 1–10 keV/μm. They could be very promising in radionuclide targeted therapy for metastatic and disseminated diseases [5].

As a heavy lanthanide, ^{165}Er shares chemical properties and can be radiolabelled with the same biologic targeting vectors already used to deliver ^{177}Lu or ^{161}Tb [6]. Moreover, ^{165}Er ($T_{1/2}$ = 10.36 h) is a great candidate for Auger-electron therapy (46.7 keV (21.6%), 47.55 keV (38.4%), 53.70 keV (3.97%) 53.88 keV (7.69%) and 55.29 keV (2.58%)) that might be produced by several routes in accelerators. Deuteron induced route ^{nat}Ho(d,2n)^{165}Er [7] has been studied due to the fact that it achieves a higher excitation function than ^{165}Ho(p,n)^{165}Er reaction [8]. Moreover, other indirect production routes have been studied such as ^{nat}Er(d,xn)^{165}Tm → ^{165}Er [9] or ^{nat}Er(p,xn)^{165}Tm → ^{165}Er [10] for the production of ^{165}Er.

International organizations advocate exploring new ways and using new facilities to produce radioisotopes for medical purposes as a complementary option to conventional methods based on nuclear reactors [11–13]. One of the reason behind is the decommissioning and ageing of existing nuclear facilities cause shortages in the supply of radioisotopes to hospitals. The production of AE emitters with highly desirable characteristics is not yet developed. Careful consideration of all parameters, including decay properties, nuclear chemistry, radiochemistry, dosimetry and radiobiology, is essential to successful design of AE-emitting radiopharmaceuticals [14,15].

IFMIF-DONES (International Fusion Materials Irradiation Facility - Demo Oriented NEutron Source) is set to become a facility aimed at irradiating materials with neutrons to characterize crucial components for future fusion reactors [16]. The final version of IFMIF will comprise two identical accelerators directing 40 MeV deuterons at the same neutron-producing target, a lithium jet target. Currently, under design and construction is DONES in Granada [17], the initial phase, will hold only one 40 MeV accelerator focusing deuterons onto the lithium jet target. The expected outstanding characteristics of DONES in terms of neutrons and deuterons have pushed the complementary applications on radioisotope production for nuclear medicine [18,19]. In this framework of expanding the applications of the facility, it is foreseen that 0.1% of the deuteron beam will be deflected for a new experimental hall.

In the present work, we determine the production of ^{165}Er at DONES with the d+^{165}Ho reaction at 40 MeV and 125 μA. Due to the high-power delivered by the deuteron beam a cooling device for the Ho sample will be studied based on an existing device for similar

* Corresponding author.
E-mail addresses: melopez@ugr.es (E. López-Melero), jpraena@ugr.es (J. Praena).

https://doi.org/10.1016/j.nme.2024.101659
Received 9 December 2023; Received in revised form 4 April 2024; Accepted 18 April 2024
Available online 20 April 2024

Table 1
Semiempirical coefficients of holmium for stopping power of protons by Ziegler [23].

Target	Bethe's stopping coefficients			
Ho	A_6	A_7	A_8	A_9
	0.03416	1640	−14.74	5.051
	A_{10}	A_{11}	A_{12}	
	−0.6117	0.03141	−0.0005801	

purposes [20,21]. This study includes thermo-mechanical analysis of the ^{165}Ho target using SolidWorks simulation software [22] of the temperature reached by the device and the sample.

2. Materials and methods

2.1. Theoretical calculations

The production of ^{165}Er is obtained from the differential equation:

$$\frac{dN_{Er}}{dt} = R_{Er} - N_{Er}\lambda_{Er} \tag{1}$$

where N_{Er} is the number of nuclei produced of ^{165}Er, R_{Er} is the production rate of ^{165}Er and λ_{Er} its decay constant. The production rate is given by:

$$R_{Er} = \frac{I}{q}\int_{E_i}^{E_f}\frac{\sigma(E)}{S^d_{Ho}(E)}dE \tag{2}$$

where $\sigma(E)$ is the reaction cross-section, $S^d_{Ho}(E)$ is the stopping power of the deuterons in Ho; I is the intensity of the deuteron beam and q is the charge of the deuterium.

The number of nuclei produced at the end of bombardment (EOB) is given by:

$$N_{Er}(t) = \frac{I(1-e^{-\lambda_{Er}t})}{q\lambda_{Er}}\int_{E_i}^{E_f}\frac{\sigma_{(d,2n)}(E)}{S^d_{Ho}(E)}dE \tag{3}$$

where $\sigma(E)$ is the (d,2n) TENDL-2021 cross-section [24] and t is the irradiation time. The integration limits are set according to the energy loss of the incoming deuterons in the production device.

The stopping power in [eV/10^{15} atoms/cm^2] is given by the semi-empirical expression developed by Andersen and Ziegler [23] for protons:

$$S^p_{Ho}(E) = \frac{A_6}{\beta^2}\left[ln\left(\frac{A_7\beta^2}{1-\beta^2}\right) - \sum_{i=0}^{4} A_{i+8}ln(E)^i\right] \tag{4}$$

where, $\beta^2 = 1-(1/(1+E/m_p))^2$, E is the proton energy in [keV/amu], m_p is the proton mass [keV/c^2] and the values of A_i are Bethe's stopping coefficients characteristic constants of the material. Table 1 shows the Bethe's stopping coefficients for holmium which are dimensionless except A_6 in [eV/10^{15} atoms/cm^2]. Then, the relation between the expression for the stopping power of deuterons and protons is:

$$S^d_{Ho}(E) = S^p_{Ho}\left(\frac{m_p}{m_d}E\right) \tag{5}$$

where m_p and m_d are the mass of a proton and deuteron in the units keV/c^2, respectively.

Regarding the cross-sections, only a few experimental works deal with deuterons induced activation products on natural Ho. Tárkányi et al. [7] investigated the ^{165}Ho(d,2n)^{165}Er excitation functions up to 20 MeV, whereas Hermanne et al. [25] investigated the cross-section for deuteron induced reactions on Ho and measured the excitation functions between 3 MeV and 50 MeV. Fig. 1 shows the results of both experimental works and calculations made with TALYS code [26] from TENDL-2021.

Finally, the theoretical specific activity of ^{165}Er can be calculated from the activity and produced mass,

$$SA_{Er}(t) = \frac{A_{Er}(t)}{m_{Er}(t)} = \frac{\lambda_{Er}(t)N_{Er}(t)}{m_{Er}(t)} \tag{6}$$

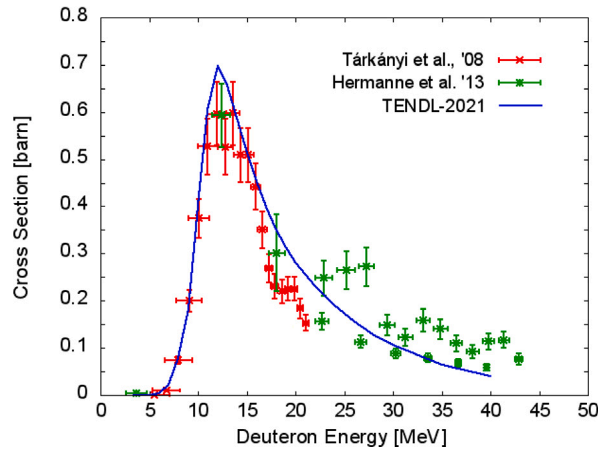

Fig. 1. Excitation functions for ^{nat}Ho(d,2n)^{165}Er nuclear reaction.

where m_{Er} is the mass of ^{165}Er, which can be calculated as: $m_{Er}(t) = N_{Er}(t)\cdot M_{at_{Er}}/N_A$.

2.2. Thermal simulations

Considering that the Ho sample will be irradiated with deuterons at 125 μA, the delivered power to the sample is an issue. Therefore, it is necessary to design a backing and cooling device for the Ho sample. In fact, the ability of the device to sustain a high-power will determine the ^{165}Er production. Here we consider backing and cooling system based on another device designed for a lithium sample for the purpose of neutron production [20]. Such device was constructed in copper with horizontal channels to circulate the cooling fluid, water. Experimental tests performed with 2.8 MeV proton beam on updated version of the device showed that 3 kW/cm^2 could be sustained keeping device below 180 °C [21].

The modification we consider here is the use of a double cooling system with the Ho sample between them, a kind of Ho sandwich. Fig. 2 shows the design of the final configuration with 7 mm thick and 45 mm width and height. It is composed of 30 "millichannels" of 1 mm diameter with 1.5 mm of separation between them. The Ho sample is located between the double cooling system, with 0.5 mm distance between the sample and the millichannels. The dimensions of the sample are 20 mm in diameter and 250 μm in thickness. The cooling fluid flows through the millichannels at 0.6 l/min and 273 K. The former parameters were obtained in a iterative process because different thicknesses of Ho sample mean different delivered powers, thus, different sample temperatures.

In order to carry out a realistic theoretical study of the ^{165}Er production, such iterative process has been performed with SolidWorks [22] which features a Computational Fluid Dynamics (CFD) tool that allows us to perform heat transfer studies and flow simulations on our system, and to estimate temperature distributions of the involved materials. We perform steady-state flow simulations where the beam profile is assumed to be parallel, uniform and with the same radius as the sample. Using SRIM code [27], the power dissipated in the sample has been estimated as a function of the input and output energy of the deuterons beam. We adjusted the device geometry so that the deuterons reach the sample with 18 MeV, the output energy is 12.9 MeV, thus, maximizing the production cross section, keeping the temperature below the melting points of the materials with 67% of transmission of deuterons due to the copper between the millichannels. Finally, the thermal contact resistance has been introduced in the simulation when the heat wave propagation reached the Cu/Ho/Cu interfaces as a value of 4 $\cdot 10^{-7}$ K m^2/W [28].

Table 2
Comparison between experimental ^{165}Er activities [8,10] and the present work at DONES. ΔE_{cp} indicates the energy range of charged particles in each case, in MeV; I is the current of the charged particle in μA; t_i is the irradiation time and t_c is the decay time in hours (only needed for indirect routes); A is the activity in MBq.

Route	ΔE_{cp} (MeV)	I (μA)	t_i (h)	t_c (h)	Activity (MBq)	Reference
^{nat}Ho(p,n)^{165}Er	16–7	1	1	0	$7.90 \cdot 10^1$	[8]
^{nat}Ho(p,n)^{165}Er	30–7	1	1	0	$1.42 \cdot 10^2$	[8]
^{nat}Er(p,xn)^{165}Tm $\rightarrow^{165}$Er	30–29.4	1	30	24	$3.59 \cdot 10^3$	[10]
^{nat}Er(p,xn)^{165}Tm $\rightarrow^{165}$Er	70–69.7	1	30	24	$1.24 \cdot 10^4$	[10]
	18–12.9	1	1	0	$(1.059 \pm 0.014) \cdot 10^2$	
	18–12.9	1	30	0	$(1.417 \pm 0.085) \cdot 10^3$	
^{nat}Ho(d,2n)^{165}Er	18–12.9	125	1	0	$(1.324 \pm 0.018) \cdot 10^4$	This work
	18–12.9	125	30	0	$(1.771 \pm 0.024) \cdot 10^5$	

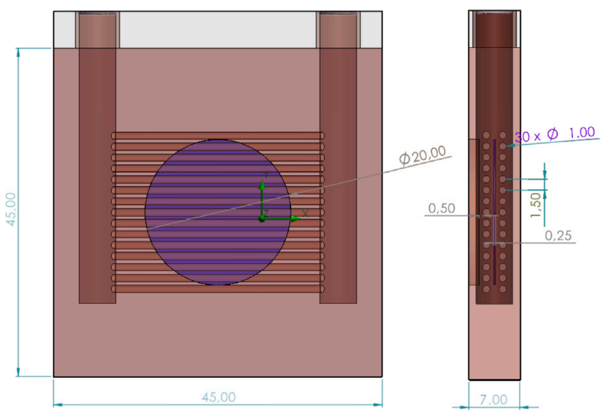

Fig. 2. Design of double water-cooled system. The copper backing is 7 mm thick and 45 mm width and height. It is composed of 30 "millichannels" of 1 mm diameter with 1.5 mm of separation between them. 15 millichannels are located in front of the holmium sample and another 15 behind it. The distance between the sample and the millichannels is 0.5 mm. The dimensions of the sample are 20 mm in diameter and 250 μm thick.

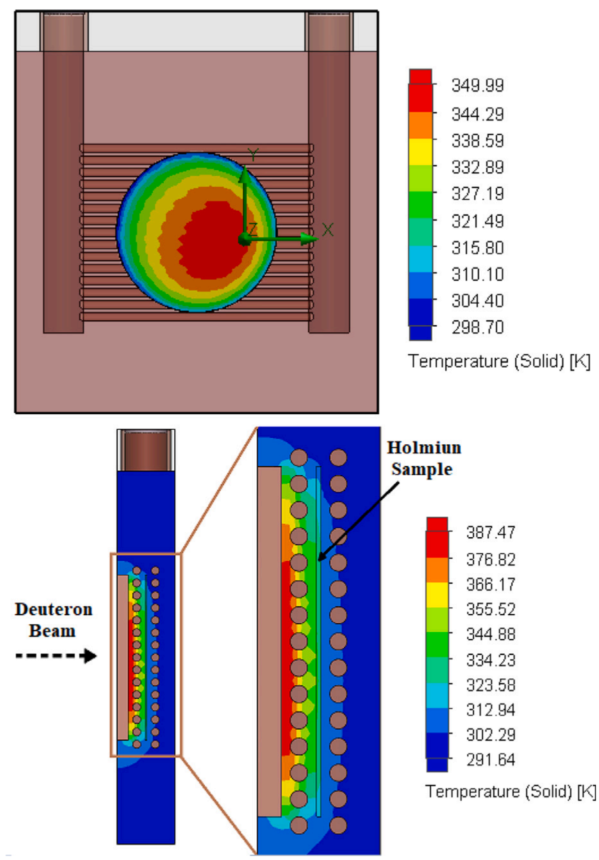

Fig. 3. Temperature distribution in the holmium sample (up). Side view of the backing and holmium sample temperature distribution (bottom).

3. Results

^{165}Er production has been calculated according to the setup discussed previously. Table 2 shows the results of production activity with deuteron compared to conventional reactions producing ^{165}Er based on cyclotrons [8,10]. For direct route, ^{nat}Ho(p,n)^{165}Er reaction, we include the most adequate energy ranges for production in conventional cyclotrons as claimed by the authors [8]. In case of the indirect routes, ^{nat}Er(p,xn)^{165}Tm→^{165}Er, also we have taken into account the decay times for ^{165}Er production [10].

^{165}Er production at low current, 1 μA, and short irradiation times, is very promising at DONES compared to conventional routes based on proton production in cyclotrons. Whereas, low currents and long irradiation times are only necessary in the case of indirect route production. The results calculated are of the same order of production, however, the energy range needed for this, in the case of deuterons, is much smaller. This would eliminate the opening of many energetically possible channels, which would generate impurities in the sample and unnecessary activation on the target. In our case, irradiation with long exposure times would not be necessary, as the ^{nat}Ho(d,2n)^{165}Er route is direct.

Finally, the production at 125 μA of current, has been studied with SolidWorks to guarantee the device's resistance to the need to dissipate high heat power. The production results would be very promising, even without the need to reach long exposure times.

Taking into account the power dissipated by the backing and the sample, flow simulations and thermo-mechanical studies have been carried out for the proposed setup. Fig. 3 shows the temperature reached by the sample and backing in steady state. The maximum temperature remains well below the melting point of Ho (1747 K) and copper (1358 K). Fig. 4 shows the fluid temperature distribution in the front face to the deuteron beam. Water cooling helps to dissipate some of the heat generated in the sample and backing. At steady state, the maximum nuclear and atomic heating density generated in the holmium sample is shown in Fig. 5.

Based on the pressure results obtained in flow simulation through the millichannels, the study has been complemented with a structural thermo-mechanical stress analysis, shown in Fig. 6. As can be seen, the Von Mises parameter that evaluates the mechanical stresses of the system, in our case, the fluid stresses and pressures, does not exceed the maximum value of the tensile strength of copper (210 MPa).

4. Conclusions

The research and development of compounds and biomolecules labelled with radionuclides obtained from rare earth elements is growing in nuclear medicine. The availability at IFMIF-DONES of 40 MeV

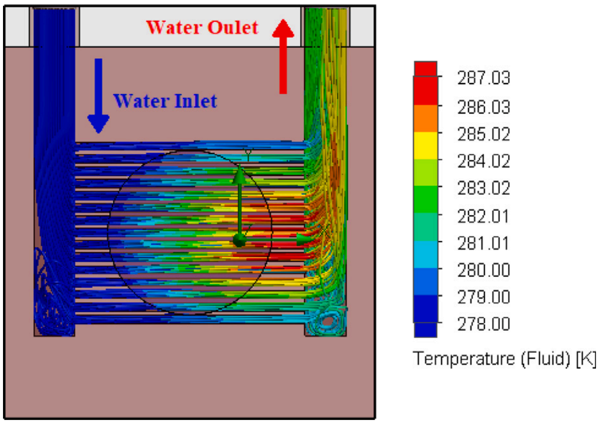

Fig. 4. Fluid temperature distribution in the front face to the deuteron beam.

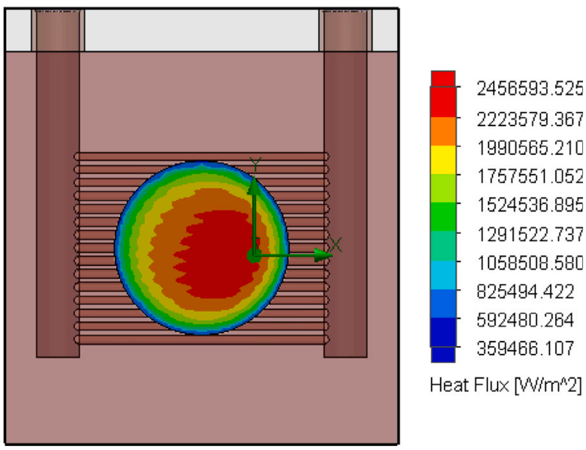

Fig. 5. Nuclear and atomic heating density generated in Ho sample. The cut plot has been made in the plane of maximum value of this parameter.

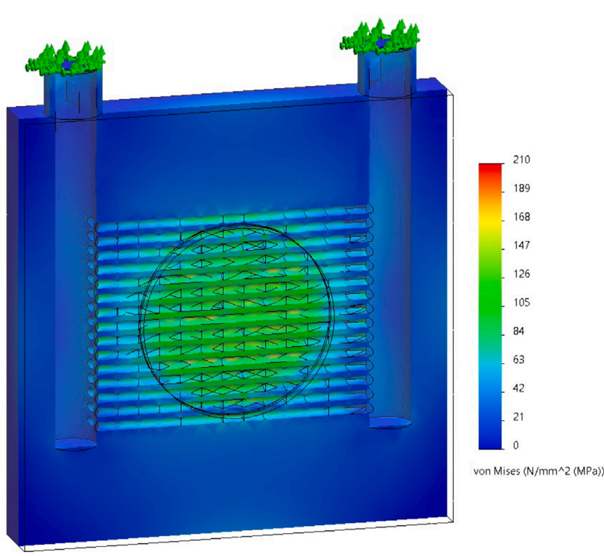

Fig. 6. Static analysis of Von Mises stresses. Cut plot of the cross section of the device.

deuteron beam at 125 μA for complementary applications provides a perfect framework for radioisotope production for nuclear medicine. Here, we have studied the production of ^{165}Er, an Auger electron emitter with promising properties.

Due to the high-power delivered by the deuteron beam at 125 μA a realistic cooling system have been simulated. Considering this device, our results show a superior activity to other direct and indirect routes. Nevertheless, at lower current (1 μA) the show production is higher or similar to other studied routes in the literature. These results push further experimental studies that we are planning to characterize possible contamination, as stable ^{164}Er and ^{166}Er, as well as the molar activity after chemical separation.

CRediT authorship contribution statement

E. López-Melero: Writing – original draft, Methodology, Investigation. **F. Arias de Saavedra:** Methodology, Investigation. **I. Da Silva:** Conceptualization. **A. Roldán:** Methodology. **J. Praena:** Writing – original draft, Methodology, Investigation, Funding acquisition, Conceptualization.

Declaration of competing interest

The authors declare that they have no known competing financial interests or personal relationships that could have appeared to influence the work reported in this paper.

Data availability

Data will be made available on request.

Acknowledgements

This work has been carried out within the framework of project PID2020.117969RB.I00 funded by MICIU/AEI /10.13039/5011000110 33. The EUROfusion Consortium funded by the European Union via the Euratom Research and Training Programme (Grant Agreement No 101052200 – EUROfusion) partially funded this work. Views and opinions expressed are however those of the author(s) only and do not necessarily reflect those of the European Union or the European Commission. Neither the European Union nor the European Commission can be held responsible for them. This work was partially supported by Spanish projects Junta de Andalucía (FEDER Andalucia 2014–2020) projects P20-00665 and B-FQM-156-UGR20, and Empresarios Agrupados Internacional, S.A. with funding from Spanish CDTI (Misiones DONES-EVO) (Contrato UGR-OTRI 5270). E. López-Melero acknowledges support from Junta de Andalucía, European Regional Development Fund (ERDF), Euratom Research and Training Programme (Grant Agreement No 101052200 – EUROfusion).

References

[1] S.P. Fricker, Chem. Soc. Rev. 35 (2006) 524.
[2] A.T. Kendi, et al., Med. Mol. Imaging 213 (2019) 309.
[3] C. Kratochwil, et al., Eur. J. Nucl. Med. Mol. Imaging 46 (2019) 2536.
[4] A.C. Camargo-Miranda, et al., Pharmaceutics 13 (2021) 971.
[5] A.I. Kassis, Radiat. Prot. Dosim. 143 (2011) 241.
[6] Da Silva, et al., Molecules 26 (24) (2021) 7513.
[7] F. Tárkányi, et al., Nucl. Instrum. Methods Phys. Res. B 266 (2008) 3529.
[8] F. Tárkányi, et al., Nucl. Instrum. Methods Phys. Res. B 266 (2008) 3346.
[9] F. Tárkányi, et al., Nucl. Instrum. Methods Phys. Res. B 259 (2007) 829.
[10] F. Tárkányi, et al., Appl. Radiat. Isot. 67 (2009) 243.
[11] Nuclear Physics European Collaboration Committee, Nuclear Physics for Medicine, ISBN: 978-2-36873-008-9, 2014, see: https://www.nupecc.org/pub/npmed2014.pdf.
[12] Nuclear Physics European Collaboration Committee, Long range plan 2017 perspectives in nuclear physics, 2017, see: https://www.esf.org/fileadmin/user_upload/esf/Nupecc-LRP2017.pdf.
[13] EUROATOM. Supply Agency of the European Atomic Energy Community, Supply of medical radioisotopes, 2021, see: https://euratom-supply.ec.europa.eu/activities/supply-medical-radioisotopes_es.
[14] J. Bolcaen, et al., J. Nucl. Med. 64 (9) (2023) 1344.
[15] Technical Meeting on Auger Electron Emitters for Radiopharmaceutical Developments, IAEA, 2022, see: https://www.iaea.org/events/evt2103627.

[16] W. Królas, et al., Nucl. Fusion 61 (2021) 125002.
[17] European Strategy Forum on Research Infrastructures, International Fusion Materials Irradiation facility - DEMO Oriented NEutron Source, 2018, see: http://www.roadmap2018.esfri.eu/projects-and-landmarks/browse-the-catalogue/ifmif-dones/.
[18] E. López-Melero, Nucl. Mater. Energy 38 (2024) 101575.
[19] J. Praena, et al., Invited Talk Int. Nuclear Data Conference 2019, in: EPJ Web of Conferences, vol. 239, 2020, p. 23001.
[20] P. Mastinu, et al., Physics Procedia 26 (2012) 261.
[21] P. Mastinu, et al., Il Nuovo Cimento C 38 (2015) 1.
[22] J. Matsson, SDC publications, 2023.
[23] H.H. Andersen, J.F. Ziegler, Pergamon Press, New York (1985).
[24] TENDL 2019 nuclear data library, 2019, Last update: Apr 16 14:30:42. see: https://tendl.web.psi.ch/tendl_2019/neutron_html/neutron.html.
[25] A. Hermanne, et al., Nucl. Instrum. Methods Phys. Res. B 311 (2013) 102.
[26] A.J. Koning, et al., 2021, see: https://tendl.web.psi.ch/tendl_2021/tendl2021.html.
[27] SRIM & TRIM, 2013, see: http://www.srim.org/ (accessed 22 April 2023).
[28] S. Orain, et al., Int. J. Heat Mass Transfer 44 (2001) 3973.